Spontaneous Formation of Hydrophobic Domains in Isolated Peptides

ARTICLE *in* THE JOURNAL OF PHYSICAL CHEMISTRY B · APRIL 2013

Impact Factor: 3.3 · DOI: 10.1021/jp401499x · Source: PubMed

THE JOURNAL OF PHYSICAL CHEMISTRY B

Article

pubs.acs.org/JPCB

Spontaneous Formation of Hydrophobic Domains in Isolated Peptides

Eric Gloaguen,*[,†,‡] Yohan Loquais,[†,‡] Jessica A. Thomas,[§] David W. Pratt,[∥] and Michel Mons[‡,†]

[†]Laboratoire Francis Perrin, CNRS, INP & INC, URA 2453, F-91191 Gif-sur-Yvette, France

[‡]Laboratoire Francis Perrin, CEA, IRAMIS, URA 2453, F-91191 Gif-sur-Yvette, France

[§] Department of Biology and Chemistry, Purdue University North Central, Westville, Indiana 46391, United States

[∥]Department of Chemistry, University of Vermont, Burlington, Vermont 05405, United States

ABSTRACT: Aromatic amino acids are known for their hydrophobicity and the active role they play in protein folding. Here, we investigate the intrinsic propensity of small peptides to form hydrophobic domains in the absence of solvent water molecules. The structures of three aromatic-rich isolated peptides, Ac-Phe-Phe-NH_2 (FF), Ac-Trp-Tyr-NH_2 (WY), and Ac-Phe-Phe-Phe-NH_2 (FFF), all in the gas phase, have been studied by infrared−ultraviolet (IR/UV) double resonance laser spectroscopy, aided by dispersion-corrected density functional theory (DFT-D) calculations. Spontaneous formation of hydrophobic domains is systematically observed, whatever the secondary structure adopted by the backbone. Various types of aromatic−aromatic arrangements have been identified and associated to specific secondary structures, illustrating the interplay between the hydrophobic clusters and the backbone. Backbone NH amide groups surrounded by aromatic rings have also been evidenced and are found to contribute significantly to the stabilization of aromatic pairs. These results suggest that the formation of aromatic clusters involving contiguous residues might be a very efficient process leading to the formation of hydrophobic domains in the early stages of protein folding, well before a hydrophobic collapse into the tertiary structure.

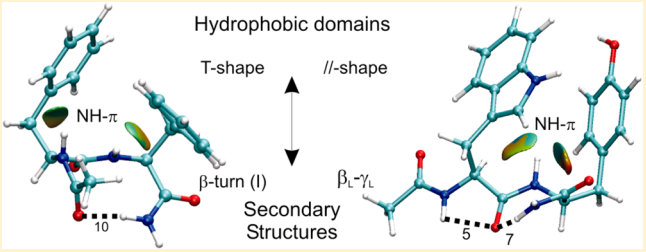

1. INTRODUCTION

The aromatic amino acids phenylalanine, tyrosine, tryptophan, and histidine play multiple roles in biological processes. Interactions between these residues are known to stabilize and shape proteins,[1−7] are ubiquitous in recognition processes,[8,9] and must be taken into consideration in drug design.[10] In folded proteins, the aromatic amino acids are often found in low permittivity domains, isolated from a generally much more polar environment.[11,12] Thus, they play a major role in the hydrophobic effect[13,14] which drives a protein to collapse into its tertiary structure. However, this collapse is often preceded and helped by the formation of small hydrophobic domains in earlier steps of protein folding,[15,16] simultaneous with the formation of secondary structure. On the scale of these small clusters, the hydrophobic effect is much less prominent,[14] leaving the role of driving force to noncovalent interactions such as van der Waals interactions. The formation of aromatic-rich hydrophobic regions in proteins or aromatic pairs in ligand−receptor complexes is thus the result of multiple interactions that are difficult to disentangle in a biological system.

In this context, gas-phase experiments have many advantages. First, from an electrostatic point of view, a vacuum approaches quite well the dielectric constant of the hydrophobic cores of proteins or any other low electric permittivity constant medium such as lipid bilayers or other crowded macromolecular environments. This is one of the reasons many biologically relevant structures have been characterized in the gas phase so far.[17,18] Structural agreement with more classical methods, like nuclear magnetic resonance (NMR) or X-ray crystallography, has been occasionally evidenced.[19] A gas-phase approach also focuses on the intrinsic properties of a molecular system by removing any effects from the solvent, hydrophobic effects included. Finally, such experiments benefit from the arsenal of accurate laser-spectroscopy techniques complemented by quantum chemistry calculations that provide powerful structural characterizations together with a comprehensive picture of the interactions at play in these systems.

Similar techniques have been used to characterize the structural and dynamical properties of prototypical aromatic systems, such as the benzene dimer. Arunan and Gutowsky[20] showed, using microwave techniques, that benzene dimer has a T-shaped geometry, with an inter-ring distance of 496 pm. Later, Hobza et al.[21] found, from ab initio (CCSD(T)) calculations, that the dimer exhibits two nearly isoenergetic structures, T-shaped and parallel displaced, a result that has been confirmed in more recent work on the protonated dimer.[22] Both binding "motifs", as well as V-type structures, are exhibited in related systems such as diphenylmethane, studied by electronic spectroscopy methods.[23,24]

Received: February 11, 2013
Revised: April 3, 2013
Published: April 4, 2013

In order to examine biologically important noncovalent interactions between hydrophobic residues, three capped peptides potentially displaying several kinds of aromatic−aromatic (ar−ar) arrangements are investigated in this paper: Ac-Phe-Phe-NH_2 (FF), Ac-Trp-Tyr-NH_2 (WY), and Ac-Phe-Phe-Phe-NH_2 (FFF). These are minimal systems capable of reproducing the ubiquitous aromatic pairs[4,25] or clusters[1,5] found in proteins. The first aim of this paper is to determine the preferred conformations of these aromatic-rich peptides in the gas phase and estimate their propensity to spontaneously form hydrophobic clusters, even in the absence of water. This is achieved by interrogating the NH and OH stretches by IR/UV double resonance spectroscopy, interpreted with the aid of quantum chemistry calculations. Such an approach has already enabled the detection of aromatic pairs in flexible molecules[26] including peptides as evidenced in one minor conformer of H-Phe-Phe-OH[27] and in the only observed conformers of Ac-Phe-Tyr(Me)-NHMe[28] and FF.[29] In order to extend the observable conformational distribution to higher-energy conformations, the original experiment on FF has been repeated in a different backing gas, a He/Ne mixture instead of Ar. This experiment revealed three new conformers of FF, which provide insight into the interplay between backbone/backbone, side chain/side chain, and backbone/side chain interactions. In addition, one conformer of WY and three of FFF have been identified. Taken together, these results show that hydrophobic domains spontaneously form in isolated peptides and that there is a diversity of interactions at play in these domains, echoing the diversity of arrangements observed in proteins.

2. METHODS

2.1. Experimental Section. Isolated peptides were formed by nanosecond-laser desorption of a sample made of peptide (GenScript Corporation) and graphite[29] in a pulsed molecular expansion of a 7:3 He:Ne gas mixture (19 bar, 1 mm diameter valve, 10 Hz). The folded peptides resulting from the cooling provided by the expansion were further analyzed by laser spectroscopy in the interaction region of a time-of-flight mass spectrometer described elsewhere.[29] UV spectra were obtained by scanning a 355 nm pumped (Nd:YAG Precision II, Continuum) BBO-doubled dye laser (400 μJ, 12 ns pulse, mildly focused, Narrowscan, Radiant Dyes) in the spectral region of the first $\pi\rightarrow\pi^*$ transition of toluene (for FF and FFF) or 3-methylindole (for WY). IR spectra were recorded using the infrared/ultraviolet (IR/UV) double resonance technique[30] by scanning the idler of a Nd:YAG pumped KTP-mounted optical parametric oscillator (OPO, 1 mJ/pulse, mildly focused, Euroscan) in the NH and OH stretch domain (2.7−3.2 μm) at a resolution of 1 cm^{-1}.

2.2. Theoretical Section. A conformational search was performed using the AMBER[31] force field included in the HyperChem Professional 7.51 package.[32] Observed conformations were then sorted according to the number and nature of intramolecular H-bonds. Only those theoretical conformations with the appropriate number and nature of H-bonds deduced from the IR spectra were optimized at the RI-B97-D/TZVPP level[33] employing the TURBOMOLE 5.10 package.[34] This DFT-D method has proven to be particularly efficient for describing interactions in isolated biological molecules.[29,35] Vibrational frequencies were obtained at the same level, in the harmonic approximation. They were further corrected using mode-dependent scaling procedures. For NH (indole) and OH (phenol) stretches, theoretical frequencies have been scaled by 0.9759, which has been chosen in order to reproduce the experimental frequencies of reference systems having a free stretch.[36,37] For backbone NH and NH_2 stretches, theoretical frequencies f_0^{th} have been corrected using scaling functions determined by comparing theoretical and experimental results obtained on a library of previously assigned peptides.[38] Theoretical scaled frequencies f^{th} were obtained using the equation $f^{th} = a \times f_0^{th} + b$ where the following set of (a,b) parameters were used; (0.92135, 188 cm^{-1}) for NH stretch, (0.63115, 1210 cm^{-1}) for NH_2 symmetric stretch (NH_2^{sym}), and (0.60872, 1324 cm^{-1}) for NH_2 antisymmetric stretch (NH_2^{anti}). Such a procedure leads to a typical agreement of $\pm$ ~20 cm^{-1} between scaled theoretical and experimental frequencies. This value is accurate enough to provide an objective assignment criterion. The NCI-plot tool[39] also was used to reveal noncovalent interactions in the assigned structures. Based on electron density and the reduced density gradient, this method is able to reveal the regions of space where the electronic density is affected by two or more partners in interaction and aims at labeling the stabilizing or destabilizing nature of the interaction.

3. EXPERIMENTAL RESULTS

3.1. FF. The upper panel in Figure 1 shows the R2PI UV spectrum of FF recorded in the spectral region of the $S_0\rightarrow S_1$ transition of toluene. IR/UV experiments revealed that this spectrum results from the overlap of the UV signature of four conformers. Conformer FF_A leads to six significant transitions in the spectrum, the two more intense being the origin transitions of both chromophores as previously observed using Ar as a carrier gas.[29] It is likely the most populated conformer as it contributes ~87% of the identified ion signal. Three additional conformers are observed using a He/Ne mixture. Conformer FF_B (~9%) is detected at 37 523 and 37 449 cm^{-1}; conformers FF_C (~3%) and FF_D (~1%) each have one transition at 37 639 and 37 577 cm^{-1}, respectively.

IR spectra of conformers FF_A, FF_B, and FF_C have been recorded using the IR/UV double resonance technique (Figure 1, lower panels). Four bands corresponding to the four NH stretch modes of the molecule have been observed in each case; values are reported in Table 1. The IR spectrum of FF_D (not shown) is noisy, and only three bands are clearly visible (3380, 3402, and 3520 cm^{-1}), making an assignment difficult.

The IR spectrum of FF_A has been previously assigned.[29] One strong C_{10} H-bond (C_n indicates a H-bond closing a n-membered ring) involving the NH_2 group is responsible for the NH_2^{anti} and NH_2^{sym} stretch which appear as the blue-most and red-most shifted bands, respectively. Two weaker NH-π H-bonds appear as a doublet slightly red-shifted compared to the NH free domain[40] (3465−3495 cm^{-1}).

Conformers FF_B and FF_C show some similarities in their IR spectra. Neither conformer has any bands in the NH-free domain suggesting that both NH groups are H-bond donors. In addition, these conformers have one band blue-shifted in the 3500−3545 cm^{-1} range which is typical of NH_2^{anti} stretch when the NH_2 group is a single H-bond donor[41] (NH_2^{anti} free in acetamide:[42] 3568 cm^{-1}). Conformers FF_B and FF_C must then be assigned to conformations with a three H-bond network.

3.2. FFF. Figure 2 (upper panel) shows the R2PI UV spectrum of FFF. It is dominated by the contribution of conformer FFF_A (~86%) with three strong transitions (37 363, 37 376, and 37 513 cm^{-1}) which are expected to be

dx.doi.org/10.1021/jp401499x | J. Phys. Chem. B 2013, 117, 4945−4955

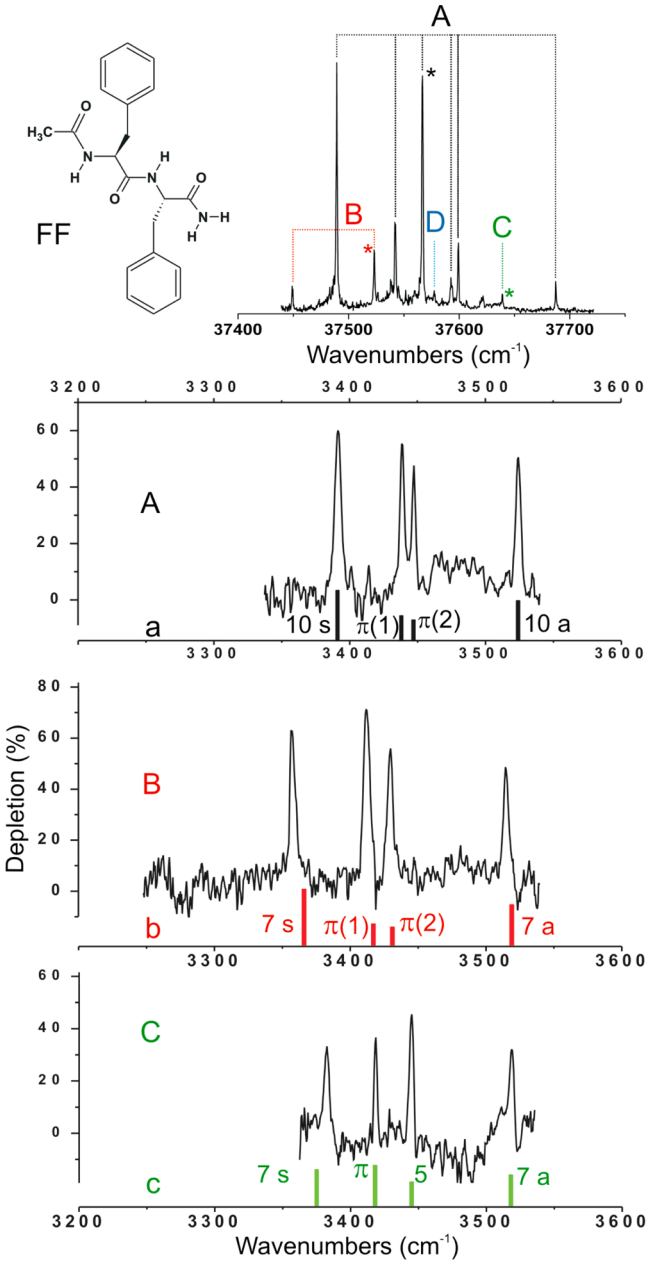

Figure 1. (Upper panel) FF molecule and its R2PI UV spectrum. Bands are assigned to one of the four identified conformers (A, B, C, and D). Asterisks mark the transition where IR spectra from IR/UV experiments have been recorded. (Lower panels) Conformer-selective IR spectra of conformers A, B, and C of FF. Stick spectra of theoretical conformers a, b, and c are presented for comparison purposes. The type of intramolecular H-bond (closing a 5-, 7-, or 10- member ring) responsible for the spectral position of the NH stretch and NH_2 symmetric (s) and antisymmetric (a) is also shown. The rank (1, 2, ...) of the NH group along the peptide chain is specified between brackets for ambiguous cases.

the origin transitions of the three separate UV chromophores, shifted slightly owing to their interactions with their environment (37 477 cm^{-1} in toluene[43]). Two other minor conformers FFF_B (~9%) and FFF_C (~5%) were also detected at 37 544 and 37 314 cm^{-1}, respectively. Other weak bands can be seen in this spectrum and could be ascribed to transitions of the other UV chromophores in these conformers. Unfortunately, they were not observed with sufficient signal-to-noise to permit analysis by IR/UV spectroscopy.

The IR spectra of the major conformers of FFF are shown in Figure 2 (lower panels). All of them have one band in the 3500−3545 cm^{-1} region, signaling a single H-bond donor NH_2 group. FFF_C has one band in the NH-free domain (3465−3495 cm^{-1}) and must then be assigned to a three H-bond network structure. FFF_A and FFF_B have no bands in the NH free domain (3465−3495 cm^{-1}), but they each have one band close to this domain at 3452 and 3459 cm^{-1}, respectively. The red-shift relative to the NH free region is not strong enough, however, to be unambiguously assigned to the weakest H-bonds reported so far in these compounds, namely, NH-π or C_5 bonds expected below 3450 cm^{-1}. FFF_A and FFF_B conformers may then be attributed to three or four H-bond network structures.

3.3. WY. Figure 3 (upper panel) shows the R2PI spectrum of WY recorded by exciting the $S_0 \rightarrow S_1$ transition of the tryptophan chromophore. The origin transition is found at 34 569 cm^{-1} (34 882 cm^{-1} in 3-methylindole[44]). Several intense and well-resolved bands are observed in the red part of the spectrum, whereas to the blue the transitions become weaker and less resolved leading to congestion. The IR/UV experiments carried out on the UV transitions shown in Figure 3 (lower panel) reveal only one conformer, WY_A. The six vibrators expected in the IR region investigated are effectively observed: two NH^{amide}, two for the NH_2 group, one NH^{indole}, and one OH^{phenol}. Remarkably, this spectrum (recorded at 34 593 cm^{-1}) shows that none of these groups is free. The band at 3631 cm^{-1} must be assigned to the slightly red-shifted OH^{phenol} stretch (free:[37] ~3659 cm^{-1}). Two bands (3500 and 3514 cm^{-1}) lie in the 3500−3545 cm^{-1} range: one must be assigned to the slightly red-shifted NH^{indole} stretch (free:[36] 3525 cm^{-1}), the other to the $NH_2{}^{anti}$ stretch of a single H-bond donor NH_2 group. This IR spectrum thus corresponds to a conformation with five H-bonds.

4. CONFORMER ASSIGNMENT

Experimental and theoretical results are compared in Tables 1, 2, and 3 for FF, FFF, and WY, respectively. The agreement between vibrational frequencies is the first criterion considered for assignment. Theoretical conformations are thus ranked according to increasing values of δ^{max}. A typical frequency agreement is reached when $\delta^{max} \leq$ ~20 cm^{-1} according to previous studies on dipeptides (see Methodology section of ref 38), although larger discrepancies have been observed for more complex systems like monohydrated peptides.[45] Thus, conformations with up to $\delta^{max} <$ 25 cm^{-1} will be given greatest consideration. δ^{RMS} is also presented to estimate how close the theoretical structure is from the experimental one: a typical δ^{RMS} below ~10 cm^{-1} suggests a good structural agreement. The second criterion that can be used consists of connecting relative energies with experimental abundances. The validity of this criterion relies on the hypotheses that all conformations are detected with comparable efficiencies and that the experimental conformational temperature is known. The first hypothesis can be invalidated when the lifetime of the excited state is significantly shorter than the laser pulse, weakening the signal potentially out of range of our setup. The first $\pi\pi^*$ state of phenylalanine is generally long-lived, although it has been evidenced that the environment of the UV chromophore can potentially shorten the lifetime down to few nanoseconds.[46] However, this effect is not expected to be strong enough to

dx.doi.org/10.1021/jp401499x | J. Phys. Chem. B 2013, 117, 4945−4955

Table 1. Assignment Table of FF[a]

FF conformers	vibrational frequencies (cm^{-1})				δ^{max} (cm^{-1})	δ^{RMS} (cm^{-1})	ΔH (0 K) (kJ mol^{-1})	ΔG (300 K) (kJ mol^{-1})	H-bond network
A (exp)	**3391**	**3438**	**3447**	3524				**0**	**3 H-bonds**
a	3395	3437	3450	3527	4	3	0	0	π-π-10
e	3385	3433	3446	3520	6	4	18	13	5-π-7
f	3374	3437	3440	3521	17	7	13	10	π-π-10
g	3415	3424	3445	3541	24	14	28	24	5-π-π
h	3415	3444	3454	3530	24	11	42	41	π-π^b-π
c	3375	3414	3449	3524	24	11	12	11	5-π-7
b	3366	3417	3431	3519	25	17	15	15	π-π-7
B (exp)	**3357**	**3412**	**3430**	3514				**6**	**3 H-bonds**
b	3366	3417	3431	3519	9	5	15	15	π-π-7
c	3375	3414	3449	3524	19	12	12	11	5-π-7
f	3374	3437	3440	3521	25	14	13	10	π-π-10
i	3365	3440	3442	3521	28	13	14	15	5-π-7
e	3385	3433	3446	3520	28	17	18	13	5-π-7
j	3355	3444	3446	3512	32	13	13	7	5-π-7
k	3351	3446	3449	3515	34	12	29	23	5-π-7
C (exp)	**3382**	**3418**	**3445**	3518				**8**	**3 H-bonds**
c	3375	3414	3449	3524	7	5	12	11	5-π-7
e	3385	3433	3446	3520	15	5	18	13	5-π-7
b	3366	3417	3431	3519	16	8	15	15	π-π-7
f	3374	3437	3440	3521	19	9	13	10	π-π-10
a	3395	3437	3450	3527	19	11	0	0	π-π-10
i	3365	3440	3442	3521	22	11	18	13	5-π-7
j	3355	3444	3446	3512	27	15	13	7	5-π-7

[a]For each observed conformer A, B, and C of FF, this table presents the experimental frequencies f_i^{exp}, their relative energies ΔG (300 K) deduced from the abundances measured on the UV spectrum assuming a conformational temperature[47] of 300 K, and the number of H-bonds according to the IR spectra (see text). For each theoretical conformation, *a*, *b*, *c*, ..., scaled theoretical frequencies f_i^{th} are given together with, $\delta^{max} = Max(|f_i^{exp} - f_i^{th}|)$, $\delta^{RMS} = (\sum_i (f_i^{exp} - f_i^{th})^2/i)^{1/2}$, the relative enthalpy at 0 K ΔH (0 K), the relative free energy at 300 K ΔG (300 K), and the nature of the H-bond network specifying the status of each NH group along the peptide chain: 5, 7, 10, or 13 indicates NH involved in intramolecular H-bond closing a 5-, 7-, 10-, or 13-member ring, respectively; π stands for NH-π H-bonds; π^b specifies NH pointing to π electrons located on the backbone; X marks the NH groups that can be considered free. For each experimental conformer, theoretical conformations are ranked according to the frequency agreement corresponding to the lowest δ^{max}.

overturn the conformational distribution, especially for multichromophoric species where the chance to properly detect one conformation is increased by the number of $\pi \rightarrow \pi^*$ transitions. Regarding the second hypothesis, laser desorption experiments have proven to produce conformational distributions reflecting high temperature equilibrium (300−450 K),[47,48] but it is unfortunately not possible to narrow this window in order to improve the comparison with theory. The criterion about energetics is then questionable and must then be used with caution in the assignment procedure.

For FF and WY, the conformational landscape is small enough to have a very limited number of conformations with both a small δ^{max} and the correct number of H-bonds deduced from the IR spectra. For WY, there are only two conformations, WY_a and WY_b, exhibiting five H-bonds, with respective δ^{max} of 22 and 69 cm^{-1} (Table 3). The assignment of WY_A to WY_a is then straightforward.

The assignment table of FF_B (Table 1) exhibits two conformations, FF_b and FF_c, with δ^{max} < 25 cm^{-1} that have to be considered for assignment purposes. However, their H-bond network differs by the substitution of an NH−π (3431 cm^{-1}) in FF_b by a C_5 (3449 cm^{-1}) in FF_c. The experimental value (3430 cm^{-1}) is typical of an NH−π bond, whereas it would correspond to an unusually red-shifted C_5 H-bond that is not reproduced in the FF_c conformation. FF_B must then be assigned to FF_b.

Only four conformations, FF_c, FF_e, FF_f, and FF_i, have to be considered in the attribution of FF_C if one excludes the conformations already attributed. In all of these conformations, the band observed at 3418 cm^{-1} is assigned to an NH-π bond. However, the unusually large red-shift for this kind of interaction is only well-reproduced in FF_c (3414 cm^{-1}), whereas it is predicted in a more classical range for NH−π bonds in the other conformations (3433−3440 cm^{-1}). FF_c is then the only conformation capable of faithfully reproducing the signature of FF_C.

The case for FFF is more complex as suggested by the length of the assignment table (Table 2). One can see that the number of conformations with δ^{max} < 25 cm^{-1} is higher than for the dipeptides. This is especially true for conformer A for which the number of H-bonds has not been clearly determined by the IR spectrum, increasing the number of conformations to consider for assignment. In addition, it has a very common IR signature that could fit many different kinds of H-bond networks. Consequently, there are 38 conformations with δ^{max} < 25 cm^{-1} that need to be taken in consideration for attribution.

To go further in the assignment process, one needs to discuss the energetics. FFF_A is the most abundant conformer detected and is then likely to be among the most stable conformations. Only two conformations out of the 38 candidates fulfill this criterion; FFF_z and FFF_a (ΔG (300 K) < 8 kJ mol^{-1}). The band observed at 3452 cm^{-1} would then

dx.doi.org/10.1021/jp401499x | J. Phys. Chem. B 2013, 117, 4945−4955

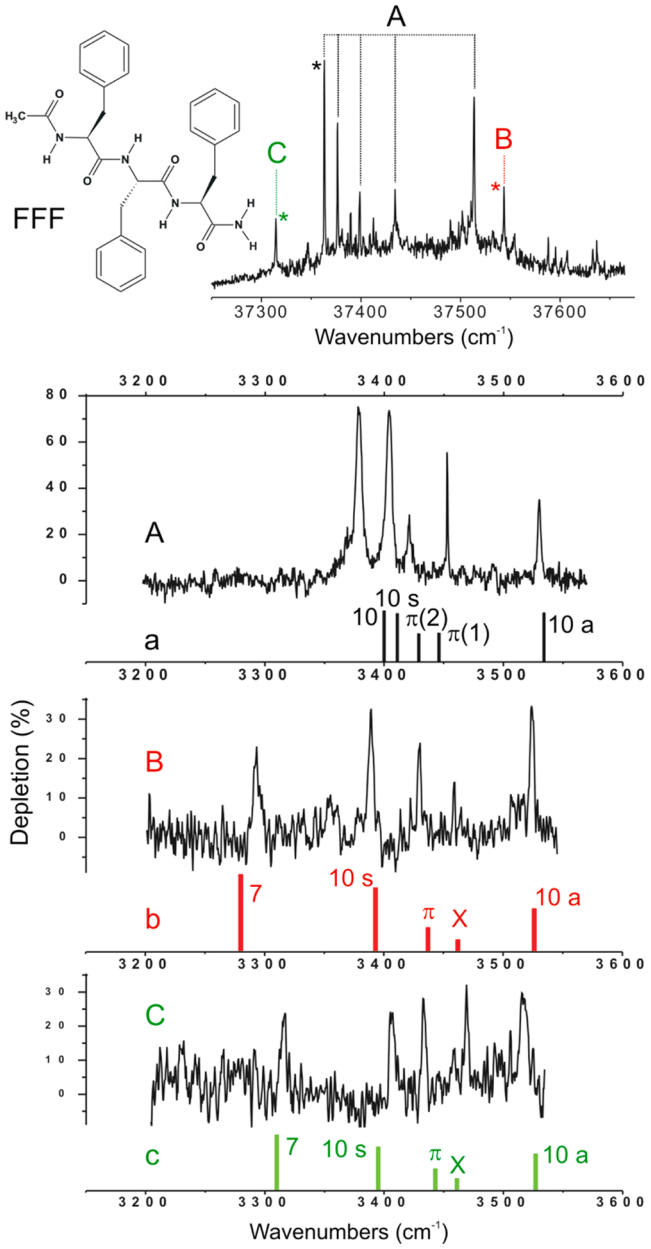

Figure 2. Results obtained on FFF for which three conformers have been identified (cf. legend of Figure 1).

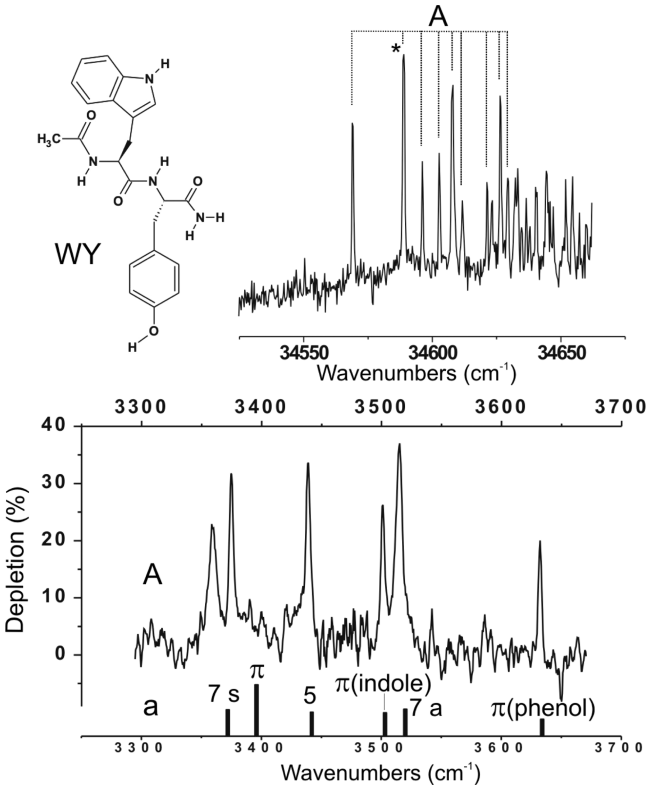

Figure 3. Results obtained on WY for which only one conformer has been identified (cf. legend of Figure 1).

be assigned either to a weak NH-π band (FFF_a 3446 cm^{-1}), or to a free NH group unusually red-shifted and not reproduced by theory (FFF_z, 3470 cm^{-1}). FFF_z is thus not a good candidate to be assigned to FFF_A. The best assignment of FFF_A is then FFF_a. Alternative assignments would involve conformations with ΔG (300 K) $\geq$ 8 kJ mol^{-1} which are unlikely to contribute to 86% of the UV spectrum but cannot be totally excluded for the reasons mentioned earlier.

According to the assignment table (Table 2), 10 conformations potentially fit the IR spectrum of conformer FFF_B (δ^{max} < 25 cm^{-1}). As discussed above, the band at 3459 cm^{-1} can either be free and unusually red-shifted or involve an unusually weak H-bond. This is clearly not the case in conformations FFF_aw, FFF_ax, and FFF_ay, where typical NH-π bonds are observed at 3437 and 3446 cm^{-1}, as well as in conformation FFF_az, where the NH free bond is found at 3481 cm^{-1}. Among the remaining six conformations, three have ΔG (300 K) higher than 29 kJ mol^{-1} (FFF_at, FFF_au and FFF_av), making their existence in measurable proportion in the experimental setup very unlikely. The three conformations left, FFF_b, FFF_c and FFF_ba, are all X-7-π-10 structures. In addition, if one examines the type of the γ-turn (L or D depending on its chirality) and the β-turn (I, I′, II, II′, etc., depending on the values of the four Ramachandran angles Φ_1, Ψ_1, Φ_2, Ψ_2),[49] all three conformations have a X-7L-π-10(I) structure. They only differ by the phenyl side chain orientations, respectively g-g-g+, g-g+g+, and ag-g+ (each phenyl side chain is labeled according to the value of the $NC^{\alpha}C^{\beta}C^{\gamma}$ dihedral angle, (g±) if it lies between 0 and ±120° and (a) otherwise).[50] FFF_B is therefore very likely a X-7L-π-10(I) structure, the uncertainty being on the orientation of the two first phenyl side chains. Without further experimental evidence regarding the orientation of the aromatic rings, FFF_b can be seen only as the most probable candidate for the assignment of FFF_B as it gives the best fit to the IR data.

Similar energetic arguments lead to the consideration of only three candidates for FFF_C: FFF_c, FFF_ba, and FFF_be. All of these structures have a X-7L-π-10(I) H-bond network which can be assigned to FFF_C. Side chain orientations of FFF_C remain uncertain; g-g+g+ (FFF_c) or ag-g+ (FFF_ba and FFF_be). Among these conformations, FFF_c best fits to the IR data and can be considered as the most likely candidate for assignment.

The assignment of the FFF conformers is then not as firm as for FF and WY and remains ambiguous. There are limits of such an approach when the size of the system increases.

dx.doi.org/10.1021/jp401499x | J. Phys. Chem. B 2013, 117, 4945−4955

Table 2. Assignment Table of FFF[a]

FFF conformers	vibrational frequencies (cm^{-1})					δ^{max} (cm^{-1})	δ^{RMS} (cm^{-1})	ΔH (0 K) (kJ mol^{-1})	ΔG (300 K) (kJ mol^{-1})	H-bond network
A (exp)	**3378**	**3404**	**3420**	**3452**	3530				**0**	**3 or 4 H-bonds**
d	3376	3409	3427	3444	3531	8	5	45	31	π-π-10-10
e	3379	3395	3418	3448	3522	9	5	36	29	π-π-7-7
f	3387	3410	3423	3453	3520	10	6	14	13	S-π-π-10
g	3386	3401	3431	3449	3527	11	6	33	25	π-7-π-10
h	3389	3395	3420	3461	3527	11	6	23	20	X-π-10-10
i	3368	3393	3418	3460	3527	11	7	24	18	X-π-10-10
j	3383	3414	3432	3448	3534	12	7	25	17	π−π-10−10
k	3390	3413	3428	3456	3527	12	7	10	8	S-π−π-7
l	3376	3404	3424	3440	3531	12	3	11	8	π-π-10-10
m	3385	3413	3431	3440	3537	12	9	27	14	π-π-10-10
n	3373	3401	3433	3457	3531	13	5	31	26	X-π-10-10
o	3391	3394	3424	3459	3527	13	7	22	19	X-π-10-10
p	3379	3395	3427	3439	3522	13	7	34	27	π-π-π-7
q	3393	3409	3422	3438	3536	15	8	24	22	π-π-10-10
r	3385	3419	3427	3442	3522	15	9	19	17	S-π-π-10
s	3380	3417	3436	3452	3523	16	8	18	15	S-π-π-10
t	3394	3398	3430	3447	3523	16	9	45	31	π-π-10-10
u	3384	3420	3437	3439	3528	16	11	26	29	S-π-π-10
v	3386	3421	3432	3437	3525	17	11	19	13	π-π-π-10
w	3371	3411	3439	3462	3533	19	9	37	26	π-X-10-10
x	3385	3423	3437	3456	3519	19	11	19	22	π-π-X-13
y	3359	3409	3431	3434	3535	19	12	20	17	π-π-10-10
z	3363	3394	3440	3470	3527	20	13	8	2	X-7-π-10
aa	3398	3420	3432	3441	3532	20	12	15	18	S-π-π-10
ab	3394	3399	3441	3454	3520	21	11	37	27	π-π-10-10
ac	3386	3415	3441	3456	3538	21	10	11	12	X-π-10-10
ad	3378	3421	3441	3458	3540	21	11	22	18	π-π-10-π
ae	3400	3417	3427	3442	3532	22	11	25	21	S-π-π-10
a	3400	3411	3429	3446	3534	22	10	0	0	π-π-10-10
af	3356	3416	3431	3448	3536	22	11	25	21	π-π-10-10
ag	3401	3415	3429	3449	3538	23	11	9	8	π-π-10-10
ah	3370	3427	3440	3457	3512	23	15	21	27	π-π-X-13
ai	3401	3413	3431	3434	3537	23	14	23	13	π-π-10-10
aj	3391	3410	3444	3450	3537	24	10	20	21	π-π-10-10
ak	3380	3416	3444	3450	3522	24	9	18	12	S-π-π-10
al	3402	3406	3440	3457	3530	24	10	28	21	π-X-10-10
am	3354	3396	3420	3439	3528	24	10	13	10	π-π-10-10
an	3354	3405	3432	3434	3533	24	12	20	15	π-π-10-10
ao	3359	3395	3427	3477	3521	25	14	36	36	X-7-10-10
ap	3403	3426	3428	3441	3531	25	13	17	8	π-π-π-10
aq	3403	3415	3437	3441	3536	25	14	14	9	π−π-10-10
ar	3389	3404	3445	3463	3525	25	10	22	20	S-π−π-10
as	3395	3429	3436	3439	3527	25	15	24	16	π−π-10-13
B (exp)	**3293**	**3389**	**3430**	**3459**	3523				**6**	**3 or 4 H-bonds**
at	3285	3397	3434	3461	3523	8	5	41	29	π-7-X-10
b	3280	3393	3437	3462	3526	13	6	16	7	X-7-π-10
c	3310	3395	3443	3461	3527	17	8	7	1	X-7-π-10
au	3282	3408	3439	3456	3534	19	10	47	33	π-7-X-10
av	3302	3410	3434	3460	3536	21	11	46	35	π-7-X-10
aw	3290	3387	3435	3437	3525	22	7	16	9	π-7-π-10
ax	3314	3392	3437	3437	3526	22	11	9	5	π-7-π-10
ay	3305	3367	3436	3446	3520	22	11	21	20	π-7-π-10
az	3316	3387	3426	3481	3525	23	11	37	43	X-π-10-10
ba	3314	3413	3447	3464	3527	24	14	14	12	X-7-π-10
bb	3300	3414	3450	3461	3536	25	13	34	20	X-7-π-10
C (exp)	**3315**	**3406**	**3433**	**3469**	3517				**7**	**3 H-bonds**
c	3310	3395	3443	3461	3527	11	9	7	1	X-7-π-10

dx.doi.org/10.1021/jp401499x | J. Phys. Chem. B 2013, 117, 4945−4955

Table 2. continued

FFF conformers	vibrational frequencies (cm^{-1})					δ^{max} (cm^{-1})	δ^{RMS} (cm^{-1})	ΔH (0 K) (kJ mol^{-1})	ΔG (300 K) (kJ mol^{-1})	H-bond network
ba	3314	3413	3447	3464	3527	14	8	14	12	X-7-π-10
bc	3334	3407	3450	3466	3519	19	8	40	25	X-7-π-10
av	3302	3410	3434	3460	3536	19	9	46	35	π-7-X-10
bb	3300	3414	3450	3461	3536	19	14	34	20	X-7-π-10
az	3316	3387	3426	3481	3525	19	11	37	43	X-π-10-10
bd	3335	3407	3450	3466	3519	20	8	41	32	X-7-π^b-10
be	3301	3415	3435	3465	3538	21	10	21	15	X-7-π-10
bf	3289	3416	3441	3466	3530	26	12	32	31	X-7-π-10

[a]See legend of Table 1.

Table 3. Assignment Table of WY[a]

WY conformers	vibrational frequencies (cm^{-1})						δ^{max} (cm^{-1})	δ^{RMS} (cm^{-1})	ΔH (kJ mol^{-1})	ΔG (kJ mol^{-1})	H-bond network
A (exp)	**3358**	**3374**	**3438**	**3500**	**3514**	**3631**					**5 H-bonds**
a	3372	3396	3442	3503	3520	3634	22	8	3	2	5-π-7_π-π
b	3402	3443	3474	3510	3530	3631	69	29	5	7	π-π-10_π-π

[a]See legend of Table 1.

5. DISCUSSION

5.1. FF: Interplay between the Backbone and the Hydrophobic Domains. Figure 4 shows the conformations FF_a, FF_b, and FF_c, assigned to the three observed conformers of FF: FF_A, FF_B, and FF_C. FF_a is a β-turn type I (α_L-γ_L structure characterized by the following Ramachandran angles: $\Phi_1 = -68°$, $\Psi_1 = -13°$, $\Phi_2 = -100°$, $\Psi_2 = 7°$)[51] where the aromatic rings interact according to a T-shape approaching the geometry of the benzene dimer[21] as described in a previous study.[29]

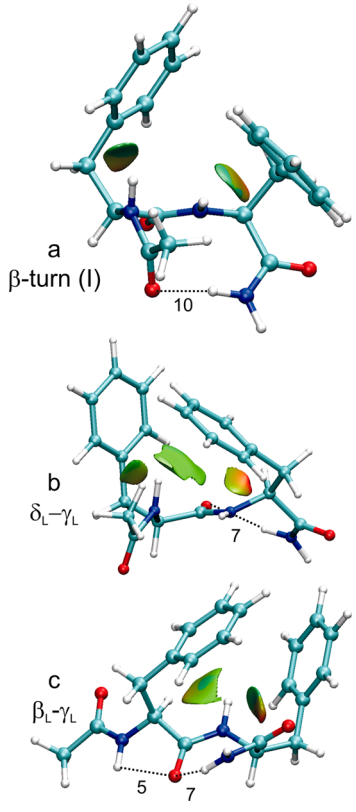

Figure 4. Conformations FF_a, FF_b, and FF_c. Dotted lines mark C_5, C_7, and C_{10} H-bonds. Interactions between NH groups and phenyl rings (NH-π interactions) are revealed by colored gradient isosurfaces provided by NCI-plot[39] (see Methods section). The type and strength of local interactions are color-coded ranging from blue for strong stabilizing interactions to red for strong destabilizing interactions. Locally weak interactions appear in green.

The backbone of FF_c adopts a β_L-γ_L structure ($\Phi_1 = -160°$, $\Psi_1 = 152°$, $\Phi_2 = -82°$, $\Psi_2 = 63°$) characterized by the well-known combination of C_5 and C_7^{eq} H-bonds.[41] The relative orientation of the phenyl rings can be seen as a face-to-face (//) or parallel-displaced arrangement.

FF_b has a backbone structure characterized by Ramachandran angles $\Phi_2 = -94°$ and $\Psi_2 = 68°$ which correspond to a γ_L-turn and $\Phi_1 = -138°$ and $\Psi_1 = 25°$ which characterize an unusual δ_L structure.[51] This conformation of the first residue is peculiar in that (i) it adopts neither of the most stable structures at the residue scale, C_5 or C_7, and (ii) it is not part of a larger intrabackbone H-bond ($C_{n>7}$). This is the first time such a δ_L-γ_L structure has been observed for a dipeptide in the gas phase. A V-shape interaction between the aromatic rings finally completes the description of this structure. It is interesting to note that the backbone structure of FF_b topologically lies between FF_a and FF_c: FF_a is transformed into FF_b by rotating mainly Φ_1 and Ψ_2, and FF_c is obtained from FF_b by rotation of Ψ_1.

Aromatic pairs are a common feature of all three observed conformers. This suggests that the ar-ar interaction plays an important role in generating the observed conformational distribution by mediating the competition between backbone structures. This is supported by the comparison with the results obtained on the Phe-Xxx[41] and Xxx-Phe[52] dipeptide series where β_L-γ_L and γ_L-γ_L structures respectively were mainly observed, and β-turns were detected as minor conformers. γ_L-γ_L structures do not allow side chain/side chain interactions, and their absence in the FF distribution can be interpreted as their relative destabilization with respect to other backbone structures where such ar-ar interactions are possible. Conversely, the δ_L-γ_L structure is generally not observed and does not even appear among the twenty lowest-energy conformations of Ac-Gly-Gly-NHMe,[53] but becomes competitive in FF probably because it allows an ar-ar interaction. These considerations suggest that the ar-ar interaction strongly controls the conformational distribution of the system.

dx.doi.org/10.1021/jp401499x | J. Phys. Chem. B 2013, 117, 4945−4955

Interestingly, one can note the variety of the relative orientations of the phenyl rings observed in this system: T-, V-, and //-shapes. Actually, the system can be seen as a benzene dimer constrained by the backbone chain. Each observed structure of the backbone imposes specific constraints, especially on the $C^{\alpha}-C^{\alpha}$ distance restricting the range of possible inter-ring distances:[3] the β-turn type I is only compatible with relatively large inter-ring distances (511 pm, T-shape) whereas β_L-γ_L forces both rings to interact at shorter distances (415 pm, //-shape) and δ_L-γ_L defines an intermediate case (469 pm, V-shape). In this last structure, both the ar-ar system and the backbone are maintained out of their respective equilibrium conformations (T- or //- shapes, and γ_L-γ_L), illustrating the subtle compromise between constraints and attractive interactions. More generally, this set of structures sheds light on the weak directionality of the ar-ar interaction between phenyl rings in peptides, echoing what has been already evidenced in the benzene dimer.[21] This contributes to the accessibility of several backbone conformations which can be interpreted as an enhancement of the backbone local flexibility brought by a strongly attractive, but poorly directional ar-ar interaction.

5.2. FF: Encapsulated NH Groups. The IR bands of FF_B and FF_C at 3412 cm^{-1} and 3418 cm^{-1}, respectively, lie in a transition region between the spectral domains signing the NH groups involved in strong H-bonds to the red (C_7, C_{10}, ...) and those involved in weak interactions to the blue (C_5, NH-π). These bands make the IR signature very discriminative, authorizing a firm assignment of the conformers (Table 1). In both FF_b and FF_c, these bands are well-predicted and assigned to an NH group pointing to the region of space located between the aromatic rings. These bands are then compatible with NH-π interactions unusually red-shifted by ~65 cm^{-1} (taking 3480 cm^{-1} as the average value for NH-free stretches), whereas typical shifts are closer to the 35−50 cm^{-1} range observed for conformer FF_A. It is even larger than the red-shift observed for the NH-π interaction in the unconstrained complex between 2-pyridone and benzene (56 cm^{-1}).[54] One can suspect that the unusual red-shifts of these NH stretches are due to the close proximity of the interacting pair of aromatic rings.

In order to reveal the interactions responsible for such a red-shift, the recently developed NCI-plot tool[39] has been used, focusing on the surroundings of the NH groups. As illustrated in Figure 4, NH-π interactions leading to typical red-shifts appear on conformer FF_a as two gradient isosurfaces between the NH groups and the aromatic rings. The plot shows that each NH interacts with only one phenyl ring at a time, making two intraresidue NH-π bonds, NH(1)-π(1) and NH(2)-π(2). However, the situation is clearly different for FF_b. While similar surfaces revealing intraresidue NH-π bonds are found, a third larger surface reveals an NH(1)-π(2) interaction. It is not possible to conclude from these plots which is the stronger interaction, NH(1)-π(2) or NH(1)-π(1). However, one can assume additive effects on NH(1) that lead to the unusual red-shift observed for its stretch. Similarly, NCI-plots reveal two interactions in conformation FF_c, NH(2)-π(1) and NH(2)-π(2), the combination of which leads to the unusual red-shift of NH(2).

5.3. WY. Figure 5 shows WY_a. It is a β_L-γ_L structure that can be directly compared to FF_c. The aromatic groups interact in a face-to-face conformation similar to the //-shape of FF_c. Unlike FF, WY is detected in only one single

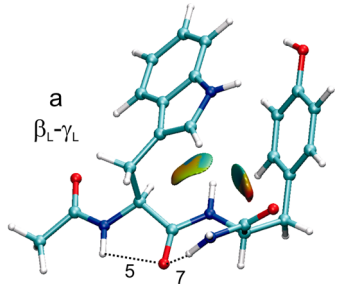

Figure 5. Conformation WY_a (cf. legend of Figure 4).

conformation, suggesting that the other β-turn and δ_L-γ_L structures are destabilized relative to the β_L-γ_L in WY. This further suggests that the ar-ar interaction is more directive in this case, favoring a face-to-face arrangement rather than a T- or V-shape interaction. One of the reasons for such a behavior might indeed be the presence of polar NH (indole) and OH (phenol) groups; the H atoms both point out of the aromatic plane, attracted by π electrons of the other aromatic group as revealed by IR spectroscopy, signing a mutual stabilization which cannot occur in a T- or V-shape.

The red-shift of the NH(2) group encapsulated between the aromatic groups is much larger (106 cm^{-1}) than previously observed in FF. NCI-plot surfaces again reveal elegantly the NH(2)-π(1) and NH(2)-π(2) interactions that are responsible for this strong red-shift. It is striking to see how an NH stretch can be as much red-shifted by two NH-π interactions as by more classical acceptors like CO groups.

5.4. FFF. The best candidates that can be assigned to FFF conformations are shown in Figure 6. These assignments suggest that the conformational distribution is largely dominated by ar-ar interactions, Phe(2) of FFF_b being the only phenyl not interacting with any other. FFF_a consists of two successive β-turns of type I. Interestingly, the two first residues reproduce the motif of FF_a. FFF_b and FFF_c are both a combination of a γ_L-turn followed by a β-turn of type I and differ mainly by the orientation of the second phenyl side-chain, g- or g+ respectively. These backbone structures have already been observed separately in different tripeptides,[55] Ac-Ala-Phe-Ala-NH_2 and Ac-Ala-Ala-Phe-NH_2. Their simultaneous observation in FFF can be attributed to the weak directionality of the phenyl−phenyl interaction which makes energetically accessible several backbone structures, provided that the ar-ar interaction is possible. It may also explain why the β_L-γ_L-γ_L previously observed[55] for Ac-Phe-Ala-Ala-NH_2 is not detected in FFF as the γ_L-γ_L sequence does not favor interactions between side chains.

6. CONCLUSIONS

This study shows that small isolated peptides provide minimalist models of hydrophobic domains in proteins. The vibrational probes of these systems provide experimental access to the interactions at play in the internal core of proteins at an unprecedented level. Several interesting features about aromatic-rich sequences emerge from this study. First, one remarkable fact is the spontaneous formation in the gas phase of conformational distributions dominated by ar-ar interactions. Consequently, these peptides fold in a way that creates regions of space where hydrophobic side chains interact with each other. These domains may be seen as hydrophobic domains or micropockets, although no water is present in the experiment

dx.doi.org/10.1021/jp401499x | J. Phys. Chem. B 2013, 117, 4945−4955

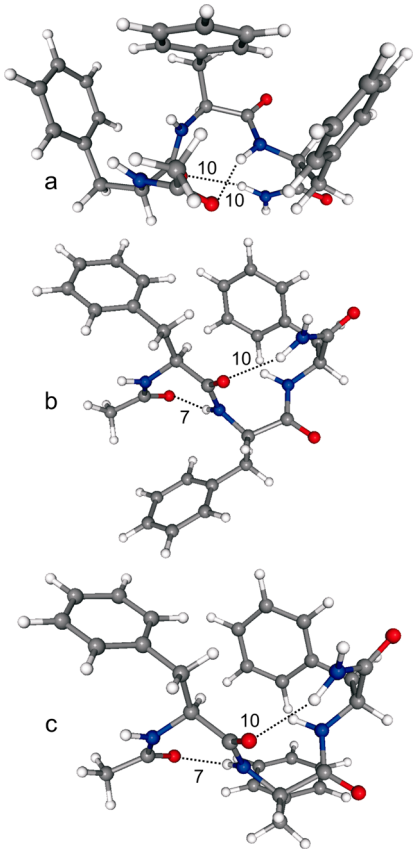

Figure 6. Conformations FFF_a, FFF_b, and FFF_c. Dotted lines mark C_7 and C_{10} H-bonds.

to generate a hydrophobic effect. As a model of hydrophobic protein chains, these systems can help us to better understand the interactions at play in larger systems. In particular, stabilizing ar-ar interactions occur for many different orientations of the aromatic rings as it has been observed in FF and FFF. This allows the backbone to adopt several energetically accessible secondary structures, suggesting an additional flexibility of the peptide chain brought by the aromatic side-chains. This is, however, not true in WY when polar groups on the side chains favor one specific orientation of the aromatic groups.

Another striking observation is the unusually strong red-shift of the IR band associated with an NH group encapsulated between two aromatic rings. This configuration shows that a polar NH group can be isolated from the vacuum and stabilized by hydrophobic groups with the same efficiency as by a classical intramolecular H-bond. The similar permittivity of vacuum and the hydrophobic cores of proteins[12] suggests that such configurations might play an active role in a biological context. Conversely, the polar NH group can also be seen as an anchor bringing two hydrophobic side chains in the same region of space to form a hydrophobic micropocket. This process could be particularly efficient, leading to the rapid formation of hydrophobic clusters in the very early steps of protein folding. While the analysis of native aromatic pairs suggests that most of them are formed in late events,[4,25] non-native clusters have also been proved to greatly affect the folding process.[56] In this context, it would be interesting to investigate the contribution of such pairs encapsulating NH groups in the kinetics of the protein folding process.

Finally, the gas phase approach used here could be applied to larger peptides and reveal other interesting features of aromatic pairing when the aromatic chains are one, two, or more residues apart in the sequence. The propensity to form hydrophobic domains in such peptides with increasing lengths would shed light on the interplay between aromatic pairing and secondary structure formation in the folding process. This type of study could bring some valuable benchmark results in order to better understand how local structural motifs are formed in the early steps of protein folding.

AUTHOR INFORMATION

Corresponding Author

*E-mail: eric.gloaguen@cea.fr.

Notes

The authors declare no competing financial interest.

ACKNOWLEDGMENTS

The authors are grateful to Dr. M.-A. Gaveau for stimulating discussions on molecular beams. E.G. would like to acknowledge M. Morgan Martin for his help with acquiring spectra on FF, and D.P. would like to acknowledge a conversation with Dr. Zan Luthey-Schulten about "foldons" which stimulated this research. Support from the French National Agency (ANR) and U.S. National Science Foundation is acknowledged (Grants ANR-08-BLAN-0158-01 and CHE-0911117).

REFERENCES

(1) Burley, S. K.; Petsko, G. A. Aromatic-Aromatic Interaction: a Mechanism of Protein-Structure Stabilization. *Science* **1985**, *229*, 23−28.

(2) Butterfield, S. M.; Patel, P. R.; Waters, M. L. Contribution of Aromatic Interactions to α-Helix Stability. *J. Am. Chem. Soc.* **2002**, *124*, 9751−9755.

(3) Chelli, R.; Gervasio, F. L.; Procacci, P.; Schettino, V. Stacking and T-Shape Competition in Aromatic-Aromatic Amino Acid Interactions. *J. Am. Chem. Soc.* **2002**, *124*, 6133−6143.

(4) Thomas, A.; Meurisse, R.; Brasseur, R. Aromatic Side-Chain Interactions in Proteins. II. Near- and Far-Sequence Phe-X Pairs. *Proteins-Struct. Funct. Genet.* **2002**, *48*, 635−644.

(5) Frank, B. S.; Vardar, D.; Buckley, D. A.; McKnight, C. J. The Role of Aromatic Residues in the Hydrophobic Core of the Villin Headpiece Subdomain. *Protein Sci.* **2002**, *11*, 680−687.

(6) Tatko, C. D.; Waters, M. L. Selective Aromatic Interactions in β-Hairpin Peptides. *J. Am. Chem. Soc.* **2002**, *124*, 9372−9373.

(7) Waters, M. L. Aromatic Interactions in Model Systems. *Curr. Opin. Chem. Biol.* **2002**, *6*, 736−741.

(8) Meyer, E. A.; Castellano, R. K.; Diederich, F. Interactions with Aromatic Rings in Chemical and Biological Recognition. *Angew. Chem., Int. Ed.* **2003**, *42*, 1210−1250.

(9) Salonen, L. M.; Ellermann, M.; Diederich, F. Aromatic Rings in Chemical and Biological Recognition: Energetics and Structures. *Angew. Chem., Int. Ed.* **2011**, *50*, 4808−4842.

(10) Martin-Gago, P.; Gomez-Caminals, M.; Ramon, R.; Verdaguer, X.; Martin-Malpartida, P.; Aragon, E.; Fernandez-Carneado, J.; Ponsati, B.; Lopez-Ruiz, P.; Cortes, M. A.; et al. Fine-Tuning the π-π Aromatic Interactions in Peptides: Somatostatin Analogues Containing Mesityl Alanine. *Angew. Chem., Int. Ed.* **2012**, *51*, 1820−1825.

(11) Kauzmann, W. Some Factors in the Interpretation of Protein Denaturation. *Adv. Protein Chem.* **1959**, *14*, 1−63.

(12) Mellor, B. L.; Cortes, E. C.; Busath, D. D.; Mazzeo, B. A. Method for Estimating the Internal Permittivity of Proteins Using Dielectric Spectroscopy. *J. Phys. Chem. B* **2011**, *115*, 2205−2213.

(13) Tanford, C. Hydrophobic Effect and Organization of Living Matter. *Science* **1978**, *200*, 1012−1018.

(14) Chandler, D. Interfaces and the Driving Force of Hydrophobic Assembly. *Nature* **2005**, *437*, 640−647.
(15) Huang, J. J.-T.; Larsen, R. W.; Chan, S. I. The Interplay of Turn Formation and Hydrophobic Interactions on the Early Kinetic Events in Protein Folding. *Chem. Commun.* **2012**, *48*, 487−497.
(16) Baldwin, R. L. Protein Folding - Making a Network of Hydrophobic Clusters. *Science* **2002**, *295*, 1657−1658.
(17) Simons, J. P. Good Vibrations: Probing Biomolecular Structure and Interactions through Spectroscopy in the Gas Phase. *Mol. Phys.* **2009**, *107*, 2435−2458.
(18) Schermann, J.-P. *Spectroscopy and Modeling of Biomolecular Building Blocks*; Elsevier: New York, 2008.
(19) Biswal, H. S.; Gloaguen, E.; Loquais, Y.; Tardivel, B.; Mons, M. Strength of NH···S Hydrogen Bonds in Methionine Residues Revealed by Gas-Phase IR/UV Spectroscopy. *J. Phys. Chem. Lett.* **2012**, 755−759.
(20) Arunan, E.; Gutowsky, H. S. The Rotational Spectrum, Structure and Dynamics of a Benzene Dimer. *J. Chem. Phys.* **1993**, *98*, 4294−4296.
(21) Hobza, P.; Selzle, H. L.; Schlag, E. W. Potential Energy Surface for the Benzene Dimer. Results of Ab Initio CCSD(T) Calculations Show Two Nearly Isoenergetic Structures: T-Shaped and Parallel-Displaced. *J. Phys. Chem.* **1996**, *100*, 18790−18794.
(22) Bandyopadhyay, B.; Cheng, T. C.; Wheeler, S. E.; Duncan, M. A. Vibrational Spectroscopy and Theory of the Protonated Benzene Dimer and Trimer. *J. Phys. Chem. A* **2012**, *116*, 7065−7073.
(23) Pillsbury, N. R.; Stearns, J. A.; Muller, C. W.; Plusquellic, D. F.; Zwier, T. S. State-Specific Studies of Internal Mixing in a Prototypical Flexible Bichromophore: Diphenylmethane. *J. Chem. Phys.* **2008**, *129*, 114301.
(24) Stearns, J. A.; Pillsbury, N. R.; Douglass, K. O.; Mueller, C. W.; Zwier, T. S.; Plusquellic, D. F. Rotationally Resolved Studies of S_0 and the Exciton Coupled S_1/S_2 Origin Regions of Diphenylmethane and the d_{12} Isotopologue. *J. Chem. Phys.* **2008**, 129.
(25) Thomas, A.; Meurisse, R.; Charloteaux, B.; Brasseur, R. Aromatic Side-Chain Interactions in Proteins. I. Main Structural Features. *Proteins-Structure Function and Genetics* **2002**, *48*, 628−634.
(26) Baquero, E. E.; James, W. H., III; Choi, T. H.; Jordan, K. D.; Zwier, T. S. Single Conformation Spectroscopy of a Flexible Bichromophore: 3-(4-Hydroxyphenyl)-N-Benzylpropionamide. *J. Phys. Chem. A* **2008**, *112*, 11115−11123.
(27) Abo-Riziq, A. G.; Bushnell, J. E.; Crews, B.; Callahan, M. P.; Grace, L.; De Vries, M. S. Discrimination between Diastereoisomeric Dipeptides by IR-UV Double Resonance Spectroscopy and Ab Initio Calculations. *Int. J. Quantum Chem.* **2005**, *105*, 437−445.
(28) Schwing, K.; Fricke, H.; Bartl, K.; Polkowska, J.; Schrader, T.; Gerhards, M. Isolated β-Turn Model Systems Investigated by Combined IR/UV Spectroscopy. *ChemPhysChem* **2012**, *13*, 1576−1582.
(29) Gloaguen, E.; Valdes, H.; Pagliarulo, F.; Pollet, R.; Tardivel, B.; Hobza, P.; Piuzzi, F.; Mons, M. Experimental and Theoretical Investigation of the Aromatic-Aromatic Interaction in Isolated Capped Dipeptides. *J. Phys. Chem. A* **2010**, *114*, 2973−2982.
(30) Gloaguen, E.; Pagliarulo, F.; Brenner, V.; Chin, W.; Piuzzi, F.; Tardivel, B.; Mons, M. Intramolecular Recognition in a Jet-Cooled Short Peptide Chain: γ-Turn Helicity Probed by a Neighbouring Residue. *Phys. Chem. Chem. Phys.* **2007**, *9*, 4491−4497.
(31) Case, D. A. *Amber 9*; University of California: San Francisco, 2006.
(32) *Hyperchem Professional 7.51*; Hypercube, Inc.: Gainesville, FL, 2002.
(33) Grimme, S. Semiempirical GGA-Type Density Functional Constructed with a Long-Range Dispersion Correction. *J. Comput. Chem.* **2006**, *27*, 1787−1799.
(34) Ahlrichs, R.; Bär, M.; Häser, M.; Horn, H.; Kölmel, C. Electronic-Structure Calculations on Workstation Computers: the Program System Turbomole. *Chem. Phys. Lett.* **1989**, *162*, 165−169.
(35) Morgado, C.; Vincent, M. A.; Hillier, I. H.; Shan, X. Can the DFT-D Method Describe the Full Range of Noncovalent Interactions Found in Large Biomolecules? *Phys. Chem. Chem. Phys.* **2007**, *9*, 448−451.
(36) Carney, J. R.; Hagemeister, F. C.; Zwier, T. S. Hydrogen-Bonding Topologies of Indole-$(Water)_n$ Clusters from Resonant Ion-Dip Infrared Spectroscopy. *J. Chem. Phys.* **1998**, *108*, 3379−3382.
(37) Inokuchi, Y.; Kobayashi, Y.; Ito, T.; Ebata, T. Conformation of L-Tyrosine Studied by Fluorescence-Detected UV-UV and IR-UV Double-Resonance Spectroscopy. *J. Phys. Chem. A* **2007**, *111*, 3209−3215.
(38) Plowright, R. J.; Gloaguen, E.; Mons, M. Compact Folding of Isolated Four-Residue Neutral Peptide Chains: H-Bonding Patterns and Entropy Effects. *ChemPhysChem* **2011**, *12*, 1889−1899.
(39) Johnson, E. R.; Keinan, S.; Mori-Sanchez, P.; Contreras-Garcia, J.; Cohen, A. J.; Yang, W. Revealing Noncovalent Interactions. *J. Am. Chem. Soc.* **2010**, *132*, 6498−6506.
(40) Chin, W.; Piuzzi, F.; Dimicoli, I.; Mons, M. Probing the Competition between Secondary Structures and Local Preferences in Gas Phase Isolated Peptide Backbones. *Phys. Chem. Chem. Phys.* **2006**, *8*, 1033−1048.
(41) Chin, W.; Piuzzi, F.; Dognon, J.-P.; Dimicoli, I.; Mons, M. Gas Phase Models of γ-Turns: Effects of Side-Chain/Backbone Interactions Investigated by IR/UV Spectroscopy and Quantum Chemistry. *J. Chem. Phys.* **2005**, *123*, 084301.
(42) Albrecht, M.; Rice, C. A.; Suhm, M. A. Elementary Peptide Motifs in the Gas Phase: FTIR Aggregation Study of Formamide, Acetamide, N-Methylformamide, and N-Methylacetamide. *J. Phys. Chem. A* **2008**, *112*, 7530−7542.
(43) Law, K. S.; Schauer, M.; Bernstein, E. R. Dimers of Aromatic-Molecules: $(Benzene)_2$, $(Toluene)_2$, and Benzene-Toluene. *J. Chem. Phys.* **1984**, *81*, 4871−4882.
(44) Carney, J. R.; Zwier, T. S. Infrared and Ultraviolet Spectroscopy of Water-Containing Clusters of Indole, 1-Methylindole, and 3-Methylindole. *J. Phys. Chem. A* **1999**, *103*, 9943−9957.
(45) Biswal, H. S.; Loquais, Y.; Tardivel, B.; Gloaguen, E.; Mons, M. Isolated Monohydrates of a Model Peptide Chain: Effect of a First Water Molecule on the Secondary Structure of a Capped Phenylalanine. *J. Am. Chem. Soc.* **2011**, *133*, 3931−3942.
(46) Mališ, M.; Loquais, Y.; Gloaguen, E.; Biswal, H. S.; Piuzzi, F.; Tardivel, B.; Brenner, V.; Broquier, M.; Jouvet, C.; Mons, M.; et al. Unraveling the Mechanisms of Nonradiative Deactivation in Model Peptides Following Photoexcitation of a Phenylalanine Residue. *J. Am. Chem. Soc.* **2012**, *134*, 20340−20351.
(47) Gloaguen, E.; de Courcy, B.; Piquemal, J. P.; Pilmé, J.; Parisel, O.; Pollet, R.; Biswal, H. S.; Piuzzi, F.; Tardivel, B.; Broquier, M.; et al. Gas-Phase Folding of a Two-Residue Model Peptide Chain: On the Importance of an Interplay between Experiment and Theory. *J. Am. Chem. Soc.* **2010**, *132*, 11860−11863.
(48) Handschuh, M.; Nettesheim, S.; Zenobi, R. Is Infrared Laser-Induced Desorption a Thermal Process? The Case of Aniline. *J. Phys. Chem. B* **1999**, *103*, 1719−1726.
(49) Hutchinson, E. G.; Thornton, J. M. A Revised Set of Potentials for β-Turn Formation in Proteins. *Protein Sci.* **1994**, *3*, 2207−2216.
(50) Chin, W.; Mons, M.; Dognon, J.-P.; Piuzzi, F.; Tardivel, B.; Dimicoli, I. Competition between Local Conformational Preferences and Secondary Structures in Gas-Phase Model Tripeptides as Revealed by Laser Spectroscopy and Theoretical Chemistry. *Phys. Chem. Chem. Phys.* **2004**, *6*, 2700−2709.
(51) Perczel, A.; Angyan, J. G.; Kajtar, M.; Viviani, W.; Rivail, J. L.; Marcoccia, J. F.; Csizmadia, I. G. Peptide Models. 1. Topology of Selected Peptide Conformational Potential-Energy Surfaces (Glycine and Alanine Derivatives). *J. Am. Chem. Soc.* **1991**, *113*, 6256−6265.
(52) Chin, W.; Dognon, J.-P.; Canuel, C.; Piuzzi, F.; Dimicoli, I.; Mons, M.; Compagnon, I.; von Helden, G.; Meijer, G. Secondary Structures of Short Peptide Chains in the Gas Phase: Double Resonance Spectroscopy of Protected Dipeptides. *J. Chem. Phys.* **2005**, *122*, 054317.
(53) Atwood, R. E.; Urban, J. J. Conformations of the Glycine Tripeptide Analog Ac-Gly-Gly-NHMe: A Computational Study

Including Aqueous Solvation Effects. *J. Phys. Chem. A* **2012**, *116*, 1396−1408.
(54) Ottiger, P.; Pfaffen, C.; Leist, R.; Leutwyler, S.; Bachorz, R. A.; Klopper, W. Strong N-H···π Hydrogen Bonding in Amide-Benzene Interactions. *J. Phys. Chem. B* **2009**, *113*, 2937−2943.
(55) Chin, W.; Piuzzi, F.; Dognon, J.-P.; Dimicoli, I.; Tardivel, B.; Mons, M. Gas Phase Formation of a 3_{10}-Helix in a Three-Residue Peptide Chain: Role of Side Chain-Backbone Interactions as Evidenced by IR-UV Double Resonance Experiments. *J. Am. Chem. Soc.* **2005**, *127*, 11900−11901.
(56) Klein-Seetharaman, J.; Oikawa, M.; Grimshaw, S. B.; Wirmer, J.; Duchardt, E.; Ueda, T.; Imoto, T.; Smith, L. J.; Dobson, C. M.; Schwalbe, H. Long-Range Interactions within a Nonnative Protein. *Science* **2002**, *295*, 1719−1722.